

Fermi National Accelerator Laboratory

FERMILAB-Conf-85/150
2563.000

THE COLLIDER DETECTOR AT FERMILAB (CDF)*

Hans B. Jensen

October 1985

*Invited talk presented at the IEEE Nuclear Science Symposium (NPS), San Francisco, California, October 23-25, 1985.

THE COLLIDER DETECTOR AT FERMILAB (CDF)

CDF Collaboration*

Presented by Hans B. Jensen
Fermi National Accelerator Laboratory+
P.O. Box 500, Batavia, Illinois 60510, U.S.A.

Abstract

A description of the Collider Detector at Fermilab (CDF) is given. It is a calorimetric detector, which covers almost the complete solid angle around the interaction region with segmented calorimeter "towers". A 1.5 Tesla superconducting solenoid, 3m in diameter and 5m long, provides a uniform magnetic field in the central region for magnetic analysis of charged particles. The magnetic field volume is filled with a large cylindrical drift chamber and a set of Time Projection Chambers. Muon detection is accomplished with drift chambers outside the calorimeters in the central region and with large magnetized steel toroids and associated drift chambers in the forward-backward regions. The electronics has a large dynamic range to allow measurement of both high energy clusters and small energy depositions made by penetrating muons. Interesting events are identified by a trigger system which, together with the rest of the data acquisition system, is FASTBUS based.

Introduction

CDF is a large detector currently being assembled at the B0 straight section of the Fermilab Tevatron. It will be used to study $p\text{-}p$ collisions at a center of mass energy of 2 TeV. The full detector is being readied for a first physics run in the fall of 1986. Parts of the detector, comprising beam-beam counters, Forward Silicon Detectors, Time Projection Chambers and scintillator calorimeters with associated electronics and readout systems were installed in the B0 Collision Hall in September 1985 for a systems test/engineering run.

An international collaboration of physicists from universities and laboratories in the U.S., Italy and Japan is responsible for design and construction of the detector. Appendix 1 identifies the collaboration.

Description of the Detector

A perspective view of the detector is shown in Fig. 1. It consists of a Central Detector and Forward-Backward Detectors. The total weight is approximately 4500 tons, half of which is in the Central Detector. The Central Detector is made such that it can be moved in one piece from the Assembly Hall to the Collision Hall on multi-ton rollers. It is connected with the control rooms via a flexible cable tray. The approximate size of the Central Detector is that of a box 9.4 m high, 7.6 m wide and 7.3 m long. Figure 2 is a photograph of the Central Detector without tracking systems and with the Endplugs removed. The bridge above the detector contains the flexible cable tray.

An overpass for the Main Ring will be constructed during the next year so that the Main Ring beam pipe

*The members and their institutions are listed in Appendix 1.

+Operated by Universities Research Association, Inc. under contract with the United States Department of Energy.

will pass above the entire detector, leaving only the Tevatron beam pipe at the center.

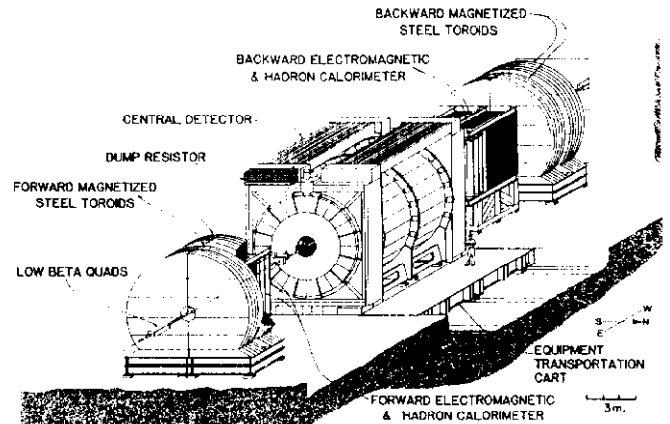


Fig. 1: Isometric drawing of CDF

The Forward-Backward Detectors remain in the Collision Hall during fixed target operations, while the Central Detector will be moved back into the Assembly Hall to prevent excessive radiation damage to the scintillator calorimeters.

A cut through one half of the detector is shown in Fig. 3. The interaction region is in the center of the detector. The rms size of the interaction region is expected to be about 30 cm along the beam direction and about 0.06 mm transverse to the beams.

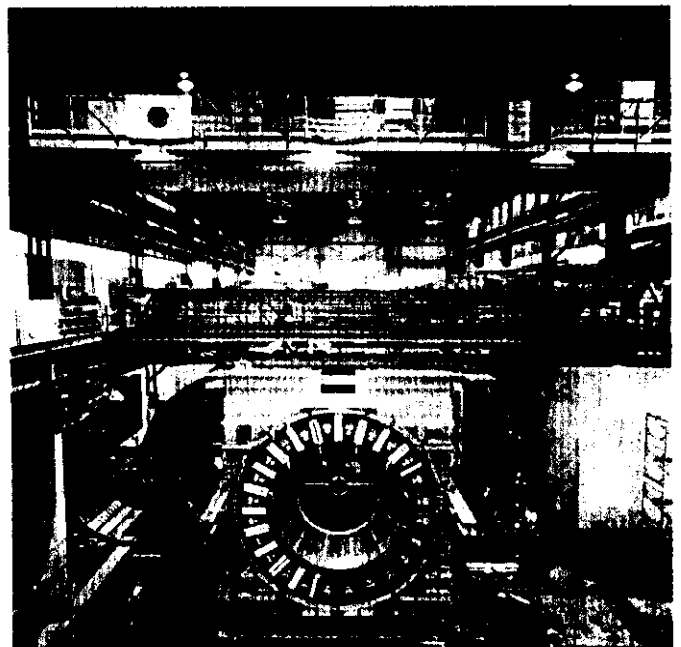
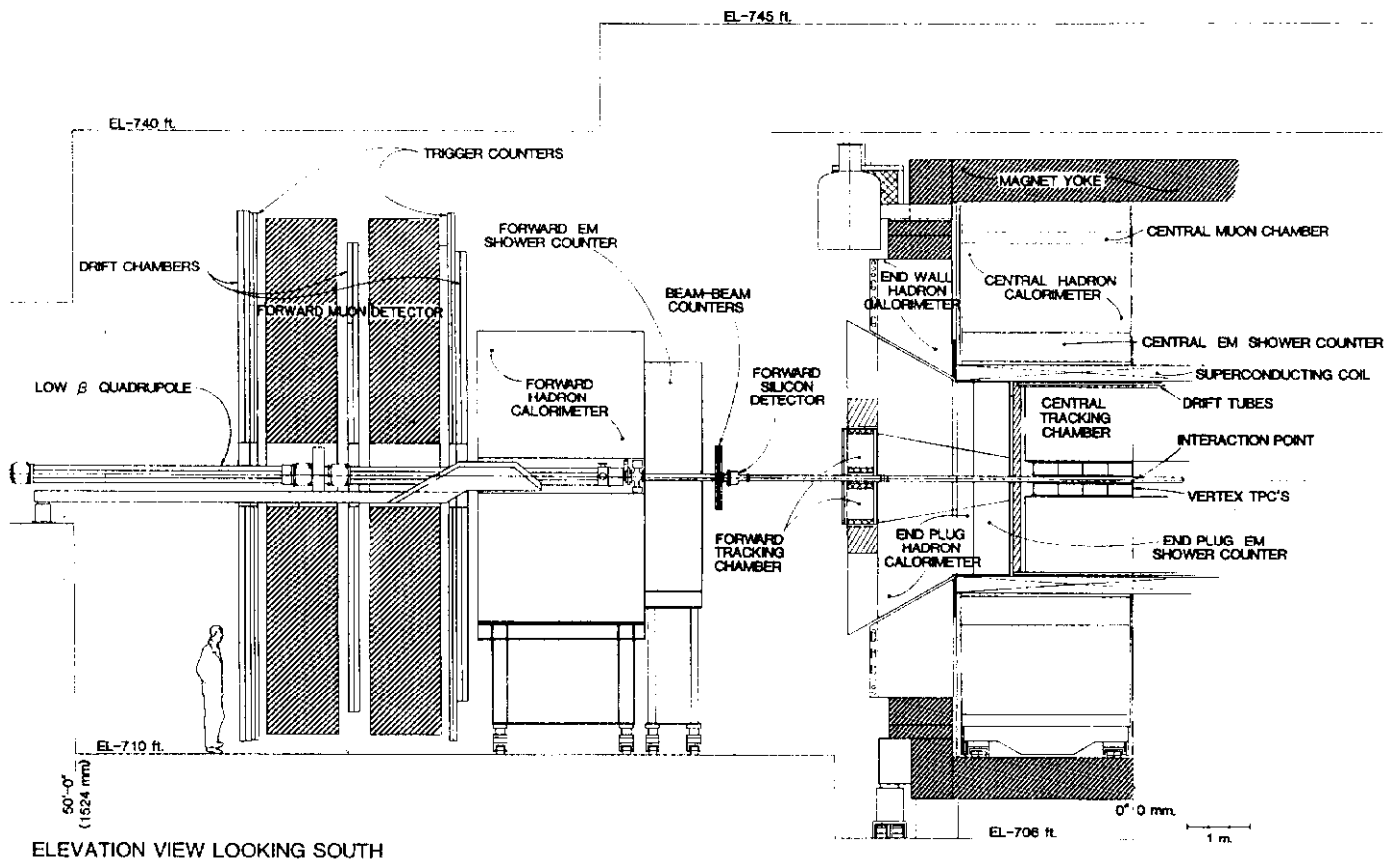


Fig. 2: The CDF Central Detector without tracking systems and Endplugs. The calorimeter "arches" are in the cabling position next to the magnet yoke.



ELEVATION VIEW LOOKING SOUTH

Fig. 3: A cut through the forward half of CDF

Magnets

The Central Detector contains a 1.5 Tesla superconducting solenoid, 3 m in diameter and 5 m long. The coil thickness, expressed in radiation lengths (X_0) is $0.85X_0$. The flux return is through the steel plates of the Endplug and Endwall hadron calorimeters. Separate steel return legs outside the central calorimeters carry the flux from end to end, as can be seen in Fig. 3. Only a minor part of the flux passes through the central calorimeter steel plates. The Forward-Backward detectors each contain two large magnetized steel toroids, 7.6 m in diameter and 1 m thick. Four coils per toroid generate a 1.8 Tesla field in the steel.

The detector components can be divided into four functional groups: Charged particle tracking, trigger counters, calorimetry and muon detection.

Charged Particle Tracking

The tracking systems are designed to measure charged particle tracks over the full solid angle. In the central region of the solenoid field, momenta are also measured. The components are:

1. A set of vertex Time Projection Chambers (vertex TPC's) to measure charged particle multiplicities over a large solid angle, and to determine accurately the z-position of the interaction vertex. If overlapping events with different vertex positions are recorded, these TPC's will be able to identify such events. They are operated at atmospheric pressure, and have been sized such that the maximum drift time is less than $3.5 \mu s$. This is the time between bunch crossings in the Tevatron when there are six proton and six antiproton bunches in the machine.

2. The Central Tracking Chamber (CTC), a large cylindrical drift chamber to measure accurately the trajectories and momenta of charged particles in the magnetic field volume. The chamber contains 84 wire layers arranged into 9 superlayers. The geometry can be seen in Fig. 4. Small angle stereo between superlayers is used for determination of the z-coordinate. The momentum resolution at a polar angle $\theta = 90^\circ$ to the proton beam is expected to be $\Delta p_T/p_T = 0.2\% \times p_T$ (in GeV/c). The chamber is operated at atmospheric pressure.

3. Drift tubes on the outside shell of the drift chamber to measure the z-coordinate of tracks with good precision using charge division.

4. Forward Tracking Chambers for measuring the trajectories of those charged particles which leave the Central Detector through the 10° hole in the Endplugs. These chambers have radial sense wires, which in a natural way continue the geometry of the axial sense wires in the cylindrical drift chamber. Each $\Delta\phi = 5^\circ$ sector contains 20 sense wires.

5. Forward Silicon Detectors inside the Tevatron beam pipe to measure small angle scattering. A Silicon Vertex Detector to measure the decay length of long-lived particles will be installed around the beam pipe inside the vertex TPC's at a later date.

Trigger Counters

1. Beam-beam counters are installed around the beam pipe in front of the Forward EM shower counters. These counters have good time resolution and determine the event time. They are also used together with the Forward Silicon Detectors as luminosity monitors.

2. Scintillator counters in the Forward Muon System are used for the muon trigger.

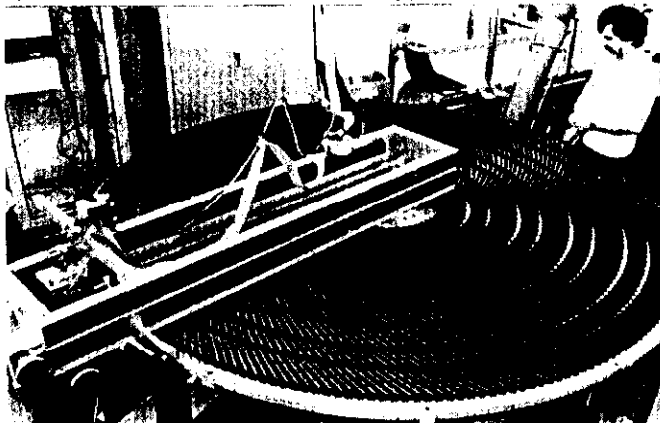


Fig. 4: Survey of wire blocks on one CTC endplate. The tilt angle of the supercells with respect to radial lines is 45° .

Calorimetry

Outside the tracking volume are electromagnetic (EM) shower counters and hadron calorimeters. All the calorimeters are of the sampling type. The EM shower counters contain lead as the absorber, whereas the hadron calorimeters have steel plates. The active medium is scintillator in the large angle region ($30^\circ < \theta < 150^\circ$) and proportional tubes at small angles to the beams ($\theta < 30^\circ$). It is known that radiation damage to scintillator occurs primarily close to the beam pipe, where the radiation dose is highest. This arrangement therefore gives some protection to the calorimeter scintillator, which is everywhere more than 1.5 m from the beams.

The calorimeters are all subdivided into many cells. Each cell is a matching "tower" or solid angle element of EM and hadron calorimeter. Such a geometry facilitates greatly the reconstruction of energy patterns in the detector for physics analysis. The angular coverage of the calorimeters is 2π in the azimuthal angle ϕ and from -4 to 4 in pseudorapidity η , which is defined as $\eta = -\ln \tan(\theta/2)$. The calorimeter tower segmentation can be represented as rectangles in the η - ϕ plane. The tower size is given by $\Delta\eta \times \Delta\phi = 0.1 \times 0.09$ (approximately) for the pad readout of the proportional tube calorimeters, while $\Delta\eta \times \Delta\phi = 0.1 \times 0.26$ for the scintillator calorimeters. The density of particles in typical inelastic collisions is more or less uniform in η - ϕ space.

In the EM shower counters, the energy resolution for 50 GeV electrons varies from about 2% at $\theta = 90^\circ$ to about 4% at small angles to the beams. In the hadron calorimeters, the energy resolution for 50 GeV charged pions varies in a similar way from about 10% (scintillator and 2.5 cm steel plates) to about 20% (proportional tubes and 10 cm steel plates). The energy dependence is approximately $1/\sqrt{E}$. Components of the calorimetry are:

1. The Central Calorimeters, consisting of calorimeter "wedges" which are built into "arches". The sampling medium is scintillator. A wedge module contains both EM shower counters and hadron calorimeters. Figure 5 shows a calorimeter arch in position next to the solenoid coil.

2. The Endwall Hadron Calorimeters, which also use scintillator. They are mounted on the steel

Endwalls of the magnet yoke, and are part of the flux return path.

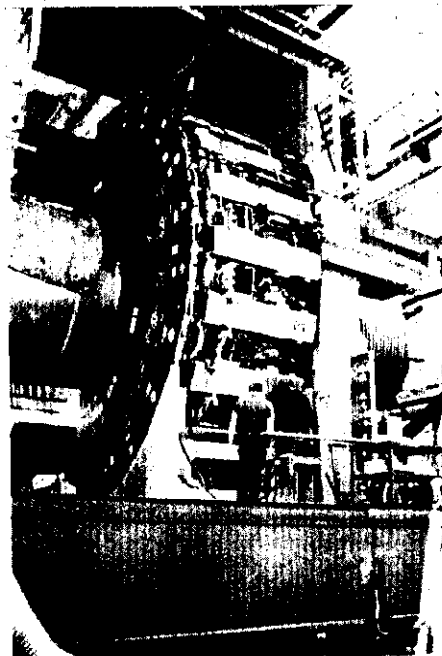


Fig. 5: A calorimeter "arch" in position on the magnet yoke next to the solenoid coil.

3. The Endplug Calorimeters, both EM and hadron calorimeters, which use proportional tubes with cathode pad readout for the energy measurement. The EM calorimeter and the first few steel plates of the hadron calorimeter are located inside the solenoid field, as can be seen in Fig. 3.

4. The Forward (-Backward) EM and hadron calorimeters, which are located between 6 m and 10 m from the interaction region on both sides of the Central Detector, also contain proportional tubes with cathode pad readout.

Muon Detection

Outside the calorimeters are muon detectors. They are:

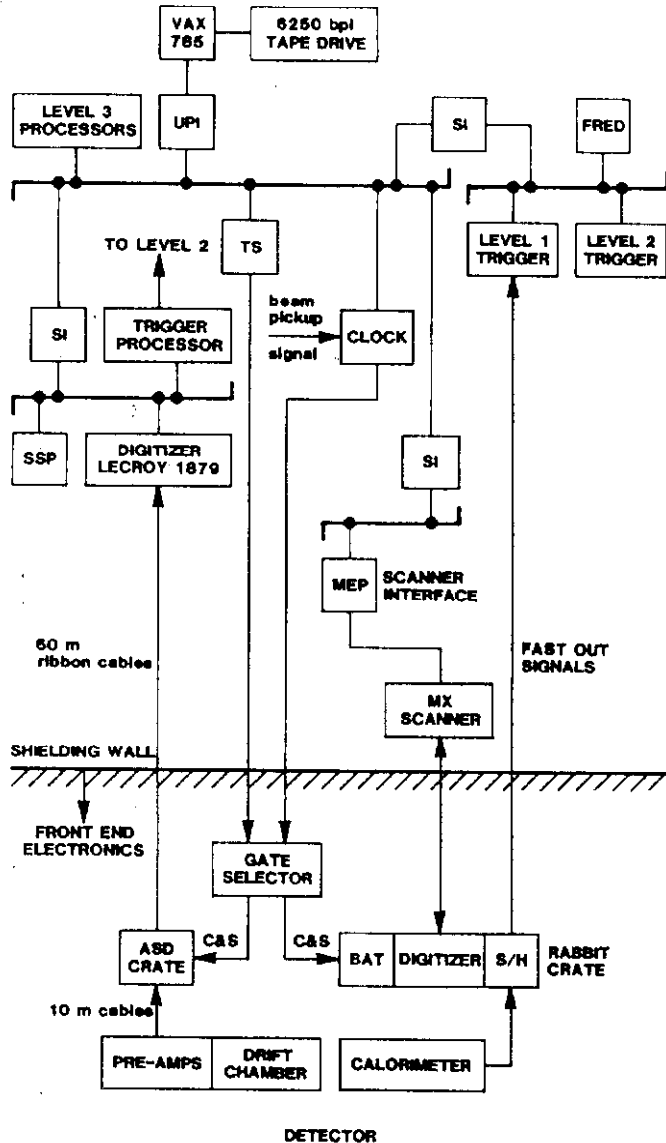
1. The Central Muon Detector. These drift chambers are located between the last two steel plates of the central wedge calorimeters. Charge division is used for determination of the z-coordinate. They are operated at high gain (limited streamer mode) to give good charge division resolution. The momentum measurement in the solenoid is expected to give a resolution of $\Delta p_T/p_T = 0.2\% \times p_T$ (in GeV/c) as for other tracks.

2. The Forward (-Backward) Muon Detectors. Each detector consists of two magnetized steel toroids and three sets of drift chambers. These drift chambers are so-called electrodeless drift chambers in which the uniform drift field is shaped by an equilibrium distribution of charges on the inside surfaces of the insulating chamber walls rather than by metallic electrodes. The expected momentum resolution is $\Delta p/p = 20\%$.

A gap currently exists in the muon detection between 17° and 50° to the beams. Upgrades to the detector to narrow this gap are being considered.

Electronics and Readout

A simplified diagram of the electronics and readout system is shown in Fig. 6. There are about 7500 electronics channels in the detector, located in approximately 150 front end electronics crates on or near the detector. There is no access to this electronics during data taking because of the potential radiation levels on the detector side of the shielding wall. The data acquisition system, consisting of VAX computers with peripherals and FASTBUS electronics is located in the control rooms. Scanners control the flow of data from the front end electronics to the FASTBUS system. A FASTBUS based trigger system is used to identify interesting events.



- UPI: UNIBUS PROCESSOR INTERFACE
- FRED: FINAL ROUTING AND DECISION LOGIC
- TS: TRIGGER SUPERVISOR
- SI: SEGMENT INTERCONNECT
- SSP: SLAC SCANNER PROCESSOR
- C&S: CLEAR AND STROBE SIGNAL
- ASD: AMPLIFIER / SHAPER / DISCRIMINATOR
- S/H: SAMPLE AND HOLD
- BAT: BEFORE-AFTER TIMING

Fig. 6: A simplified diagram of electronics and readout system.

Also located in the control rooms are high voltage power supplies for the detectors and a CAMAC based "limits and alarms" system. The high voltage distribution system is on the detector. Cables, about 60m long, connect the detector to the control rooms. These systems are now discussed briefly.

1. The RABBIT (Redundant Analog Based Bus Information Transfer) system is used for readout of calorimeters. To see how it works, consider the example of an input phototube signal, Fig. 7. A cable takes the signal from the phototube to a channel of a phototube front end card located in a RABBIT crate on the detector. A clock, synchronized to the crossing time of the stored bunches, delivers timed signals to the switches between the charge sensitive amplifier and the sample-and-hold capacitors. Their voltage is equalized after the Clear signal closes both switches. The integrated charge from the phototube is measured by the voltage difference $V_A - V_B$ because the switches are opened again just before and just after the event time, respectively. A multiplexing 16 bit ADC, also located in the crate, digitizes the information. In addition to the ADC function, the ADC card can also make pedestal subtraction and threshold comparisons, all directed by the MX scanner. The readout time per channel is dominated by the 17 μ s ADC conversion time. For phototube signals in the experiment, full scale (16 bits) is set to about 340 GeV energy, and the measured rms noise is about 20MeV, so a large dynamic range is available for measurement. For comparison, the pulse height in an EM shower counter for penetrating muons is equivalent to about 400 MeV (the value is detector dependent). It may be possible to use the x16 amplifier readout (see Fig. 7) of the average minimum ionizing particle pulse height in an EM shower counter tower as a monitor good to about 1%

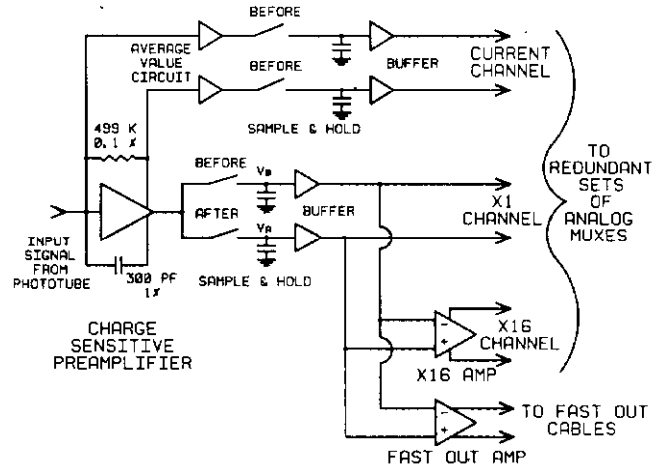


Fig. 7: One channel of RABBIT front end electronics, containing a charge sensitive amplifier for phototube signals. The Before and After switches are operated by signals derived from the Clear and Strobe (C&S) signals from the clock.

2. A different system is used for sense wire signals in the CTC and TPC's. Preamplifiers on the chambers send the signals via 10 m long cables to Amplifier-Shaper-Discriminator (ASD) crates located outside the field volume. From there, 60 m long cables carry the signals to LeCroy 1879 FASTBUS TDC crates in the counting rooms. A SLAC Scanner Processor (SSP) is the scanner for this system. The readout of the drift chambers in the Forward Muon Detector is conceptually similar.

3. The expected interaction rate is of the order

of 70 kHz at a luminosity of $10^{30} \text{ cm}^{-2} \text{ s}^{-1}$. The trigger system is used to identify the most interesting events, and to cause the data for these to be written to magnetic tape at a rate of a few Hz. The trigger system is FASTBUS based. It uses signals carried on separate cables to the control rooms. A basic input to this system consists of pulse heights from the calorimeter towers. Level 1 triggers on total (transverse) energy summed over all towers above a programmable threshold. It is deadtimeless, i.e. its decision time is less than the time between bunch crossings. Level 2 can make much more sophisticated decisions based on lists of energy clusters, high momentum track candidates in the CTC and candidate muon tracks, since tracking processors also have input to level 2. A level 2 accept causes the event information to be digitized. About 80 scanners operate in parallel to read out the digitized information. The time to read out the full detector is estimated to be a few ms. Work on a level 3 trigger system of processors with access to the digitized detector information is underway.

4. The FASTBUS system for the full detector will contain about 50 crates, linked by Segment Interconnects (SI's). More about the data acquisition system will be said below.

Detector Calibration

For calorimeters, an absolute calibration is needed to convert a measured pulse height (expressed in ADC channels) to an energy deposition in the calorimeter. A large amount of effort by the CDF groups has been put into this calibration. All calorimeter types have had their response in test beams of known energy measured as a function of incident energy, position and angle for electrons, pions or muons. In some cases, all modules of a given type have been individually calibrated. The gains at the time of calibration have been monitored by measuring the response to radioactive sources. These are, in most cases, built into the calorimeters. The absolute calibration at a later date can then be established simply by measuring again the response to these sources. The accuracy of this calibration method has been shown to be better than 1% in some cases. Through this work, a lot of knowledge and experience has been gained, not only of the calorimeters themselves, but also of the RABBIT electronics which has been used for the calibration.

The CTC is, in a certain sense, self-calibrating. By this is meant that the drift constants in the chamber can be determined from track data by virtue of the fact that all high momentum tracks will cross cell boundaries because of the 45° tilt angle of the supercells (Fig. 4). The constants are determined by demanding continuity across the boundaries. A similar method can be used in the vertex TPC's.

Systems Test/Engineering Run

Integration of the data acquisition system at B0 began early this year. The goal was to bring all the different components together at an early date in preparation for the engineering run. The system for this run was a VAX cluster, 12 FASTBUS crates, 3 SSP and 7 MX scanners and 64 partially filled front end electronics crates. The trigger was the level 1 trigger. Debugging of the system and its components was sufficiently well advanced that cosmic ray triggers could be taken and the detector read out before it was moved into the Collision Hall on September 10. An important aspect of the run was the further debugging of the trigger with stored beam in

the Tevatron and with cosmic rays. Access to the detector during the run was very limited, and it was particularly reassuring that this fact was not a problem: the electronics has proven itself quite reliable. The radiation levels were carefully monitored during the run and found to be low. The dose measured was of course position dependent, but it was less than 50 rads near the calorimeters.

Collisions in the Tevatron between protons and antiprotons at a center of mass energy of 1.6 TeV were observed with CDF on October 13. Figure 8 is a display of detector information for one of the events.

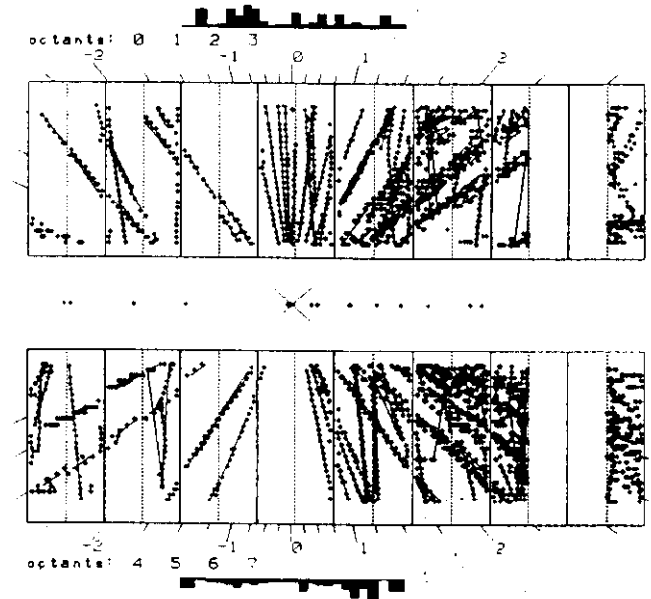


Fig. 8: A 1.6 TeV Collision as seen by the vertex TPC's. Pulse heights in the calorimeters covering the central region in this run are also indicated.

The beam pipe in this run was made of stainless steel. The wall thickness was 0.7 mm or 0.04 radiation lengths. A thinner beam pipe will be used in future runs.

Conclusion

The recent engineering run provided a realistic testing of some detector systems and of most of the electronics and data acquisition system components. The result was encouraging: Everything worked well and data could be taken. The goal for the coming ten months, during which the B0 overpass will be built, is to complete the rest of the detector. Given the current status, this should be possible. The fact that the effort to make collisions was successful this year gives us high hopes that there will be a fruitful physics run next year with a complete detector and with collisions at a center of mass energy of 1.6 TeV or higher.

Appendix 1: CDF Collaboration

F.Abe^p, D.Amidei^c, G.Apollinari^k, Y.Araiⁿ, G.Ascoli^g, M.Atac^d, V.Barnes^l, E.Barsotti^d, F.Bedeschi^{k,d}, S.Belforte^m, G.Bellettini^k, J.Bensinger^b, A.Beretasⁿ, P.Berge^d, S.Bertolucci^e, S.Bhadra^g, M.Binkley^d, C.Blocker^b, N.Bonavita^k, L.Bosisio^k, G.Brandenburg^a, A.Brenner^d, D.Brown^d, J.Buchholz^o, A.Byon^l, M.Campbell^b, R.Careyⁱ, W.Carithersⁱ, D.Carlsmith^q, T.Carroll^d, F.Cervelli^k, K.Chadwick^l, T.Chapin^m, G.Chiarelli^h, W.Chinowskyⁱ, S.Cihangir^b, D.Cline^q, T.Collins^d, D.Connor^j, J.Cooper^d, M.Cordelli^e, M.Curatolo^e, C.Day^d, R.Del Fabbro^q, M.DellaOrso^k, L.DeMortierⁱ, T.Devlinⁿ, A.Di Virgilio^l, D.DiBitonto^o, R.Diebold^a, R.Downing^g, T.Droege^k, M.Eatonⁱ, J.Elias^d, R.Elyⁱ, S.Errede^g, B.Esposito^e, A.Feldmanⁱ, E.Focardi^k, G.W.Foster^d, M.Franklinⁿ, J.Freeman^d, H.Frisch^c, Y.Fukuiⁿ, I.Gaines^d, A.Garfinkel^l, P.Giannetti^k, N.Giokaris^m, M.Giorgi^k, P.Giromini^e, L.Gladney^j, K.Goulianos^m, J.Grimson^d, C.Grosso-Pilcher^d, C.Haber^d, S.Hahn^j, R.Handler^q, R.Harrisⁱ, J.Hauser^d, Y.Hayashide^b, L.Holloway^g, B.Hubbardⁱ, J.Huth^d, M.Ito^p, J.Jaske^q, H.Jensen^d, U.Joshiⁿ, R.Kadelⁱ, T.Kamon^p, S.Kanda^p, I.Karlinger^g, H.Kautzky^d, K.Kazlauskisⁱ, E.Kearnsⁱ, R.Kephart^d, P.Kesten^b, H.Keutelian^g, Y.Kikuchi^p, S.Kim^p, L.Kirsch^b, S.Kobayashiⁱ, K.Kondo^p, U.Kruse^g, S.Kuhlmann^o, A.Laasanenⁿ, W.Li^a, T.Liss^c, N.Lockyer^j, F.Marchetto^o, M.Masuzawa^p, P.McIntyre^o, A.Menzione^k, T.Meyer^h, S.Mikamoⁿ, M.Miller^j, T.Mimashi^p, S.Miozzi², S.Miscetti^e, M.Mishinaⁿ, S.Miyashita^p, H.Miyata^b, S.Mori^p, Y.Morita^p, A.Murakami^l, Y.Muraki², C.Nelson^d, C.Newman-Holmes^a, L.Nodulman^a, J.O'Meara^d, G.Ott^q, T.Ozaki^p, S.Palanque^d, R.Paoletti^k, J.Patrick^d, N.Pearsonⁿ, R.Perchonok^d, H.Piekarz^b, R.Plunkett^m, L.Pondrom^q, J.Proudfoot^a, G.Punzi^l, D.Quarrie^d, G.Redlinger^c, R.Rezmer^a, J.Rhoades^q, L.Ristori^k, T.Rohlayⁱ, H.Sanders^c, A.Sanson^e, R.Sard^g, P.Schoessow^a, M.Schub^l, R.Schwitters^f, A.Scripano^k, S.Segler^d, M.Sekiguchi^p, P.Sestini^k, M.Shapiro^f, M.Sheaff^l, M.Shibata^c, M.Shochet^c, J.Siegristⁱ, V.Simaitis^g, J.Simmons^l, M.Sivertz^j, J.Skarha^q, D.Smith^g, R.Snider^c, S.Somalwar^d, L.Spencer^b, R.St.Denis^f, A.Stefanini^k, Y.Takaiwa^p, K.Takikawa^p, S.Tarem^b, D.Theriot^d, J.Ting^d, A.Tollestrup^d, G.Tongli^k, Y.Tsay^o, K.Turner^d, D.Underwood^a, C.vanIngen^d, R.VanBerg^j, R.Vidal^d, R.Wagner^a, R.Wagner^q, J.Walsh^j, T.Wattsⁿ, R.Webb^o, T.Westhusing^g, S.White^m, V.White^k, A.Wicklund^a, H.Williams^j, T.Winch^q, R.Yamada^d, A.Yamashita^p, K.Yasuoka^p, G.Yeh^d, J.Yoh^d, F.Zetti^l

Argonne National Laboratory^a-Brandeis University^b-University of Chicago^c-Fermi National Accelerator Laboratory^d-INFN, Frascati, Italy^e-Harvard University^f-University of Illinois^g-KEK, Japan^h-Lawrence Berkeley Laboratoryⁱ-University of Pennsylvania^j-INFN, University of Pisa, Italy^k-Purdue University^l-Rockefeller University^m-Rutgers Universityⁿ-Texas A&M University^o-University of Tsukuba, Japan^p-University of Wisconsin^q Collaboration

¹Visitor from Saga University, Japan.
²Visitor from ICRR, Tokyo University, Japan.
³Visitor from Haverford College, Haverford, PA.